

Palmprint Image Processing With Non-Halo Complex Matched filters For Forensic Data Analysis

C. Kamesh

U.G Student

Department of Information Technology

Saveetha School of Engineering, Saveetha university, Thandalam, Chennai, Tamil Nadu

Abstract— Palmprint is widely used biometric feature in biometric and forensic applications, however it is still a challenging task to process the images and extract the useful data, because the evidence, left at the crime scenes, are usually deformed and distorted by artifacts. Palmprint contains different types of visible features that can be used for identification of criminals, including big details, like crease, ridge flow, and small details, like ridges, valleys and minutiae points. In this paper we focus on ridge extraction task. We demonstrate how integration of angular preference to an existing algorithm (Non-Halo Complex Matched Filtering, NH-CMF) may significantly improve quality of extracted features. We introduce the approach where NH-CMF and automated analysis of magnitude weighted angle histogram are used for ridge pattern extraction and noise reduction. Extracted information may support or even automate ridge routing that is necessary for palmprint feature extraction in forensics.

Key words: Palmprints, forensics, image processing, CMF, NH-CMF.

I. INTRODUCTION

Palmprints share many of the discriminative features with fingerprints however they possess larger skin area and therefore provide more features to be analyzed. Palmprint recognition is widely used in biometric applications, such as access control and because about 30% of the latents recovered from crime scenes are from palms, they are also used in forensics [1]. Visible palmprint details can be subdivided into two groups: big details, like ridge flow direction and crease, and small details, like individual ridges, valleys, minutiae points (ridge endings and splits), islands and even pores on the ridges (Fig. 1) [2]. In this work we concentrate on the visible small palmprint details – individual ridges and their tracking. Since palmprint ridges appear in images as lines that are darker than the surrounding valleys, line detection algorithms may be used to extract them. State of the art techniques incorporate enhancement of the image quality by phase congruency [3], image processing with edge detection methods and conversion into binary representation by thresholding the pixel intensities [4]. Other advanced palmprint image processing techniques involve wavelets [5], Zernike moments [6] and Phase-Only Correlation [7]. Figure 1. The principal lines, ridges, and minutiae in palmprint [2] Since the images usually are distorted, simple region growing algorithm for ridge tracking cannot be used, therefore, information of several adjacent ridges becomes useful. Also, other palmprint details, like crease, usually appear one by one, not in groups of parallel lines, therefore they

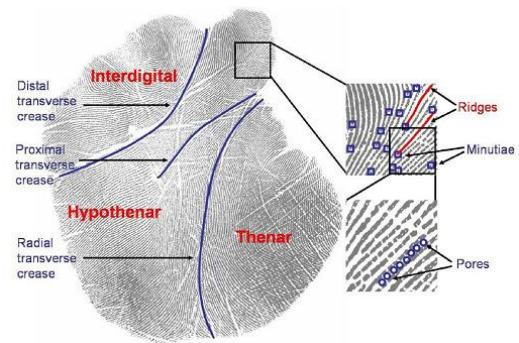


Fig. 1: Palmprint

can be distinguished from ridges. The cross section of several adjacent ridges form a pattern of repeating minimums and maximums, that can be approximated with harmonic functions, like sine wave [8]. Therefore, the transforms, based on these functions, such as 2D Fourier and Wavelet transforms [5], as well as filters, derived from them, such as Gabor filters [9], may be used to clear the unwanted noises. In this research we extend the idea of Non-Halo Complex Matched Filtering (NH-CMF) from [10], therefore, for increased clarity, this method is described in details in the next two sections. Then we present our modifications to the method and discuss the acquired results.

II. RELATED WORK

Complex Matched Filtering algorithm was introduced in [11]. Being developed for palm vein image processing in biometrics [12], it showed a simple approach for extraction of line-like objects (LLO), such as lines and edges, of arbitrary directions and even scales (latter depends on the kernel parameters). The approach was based on matched filtering and mainly presented the method of combining several matched filtering results into one, using complex coefficients. The result of CMF is a matrix of vectors $v(x, y)$ (further called as an “output image”), which has the same dimensions as the input image $f(x, y)$. Each output vector $v(x, y)$ is assigned to the corresponding pixel of the input image $f(x, y)$. Magnitude of the acquired vector $v(x, y)$ shows how similar is the pixel's neighborhood to the LLO, and the angle of this vector $Arg(v(x, y))$ shows the direction of found LLO. Therefore, not only the LLO's are extracted during CMF, but also the image is prepared for the segmentation (e. g. contour tracking) procedure. Angular information provided by the CMF, in the each image pixel, points in the direction where the next pixel of the same LLO most probably will appear. Thus, the line/contour tracking task is simplified.

However, in its initial form, the CMF had a disadvantage of producing the Halo Artifact – false vectors around the extracted regions. In [10], this problem was

investigated, the CMF method was improved and the Halo artifact appearance was eliminated. The Non-Halo CMF (NH-CMF) showed a performance that is visually comparable to the result of matched filtering, while still providing the additional information about LLO direction.

III. NON-HALO COMPLEX MATCHED FILTERING

Consider the input image $f(x, y)$ and the line detection matched filter $M(x, y; \phi_n)$, which can be rotated to arbitrary angle of

$$\phi_n = \frac{n}{N} \pi \quad (1)$$

where N is total count of used angles and $n = 0 \dots (N-1)$. Figure 2 shows the rotated kernel, which is used in this experiment (left), compared to the ridge pattern it supposed to match (right).

The cross-correlation value $s_n(x_o, y_o; \phi_n)$ of this kernel (placed with its center in pixel (x_o, y_o)) with the underlying image region is defined by the following equation: Figure 2. Filter kernel and ridge pattern to extract

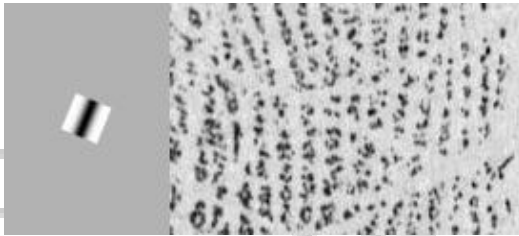


Fig. 2: Filter kernel and ridge pattern to extract

$$s_n(x_o, y_o; \phi_n) = \sum_D \sum f(x, y) \cdot M(x-x_o, y-y_o; \phi_n) \quad (2)$$

The summation of values is accomplished within the kernel boundaries D for variables x and y . To process the image according to the CMF or NH-CMF algorithm, it is first necessary to correlate the image with all possible rotated kernels, acquiring matched filtering values $s_n(x_o, y_o; \phi_n)$ for each n and in each image pixel (x_o, y_o) . Each of the N values shows the similarity between the image region around (x_o, y_o) and the kernel. This feature was exploited in [10] to prevent filter from processing negative values of correlation (which results in a Halo Artifact production), and will be exploited in this work for the other purpose. The Halo Artifact is removed by eliminating any negative values of correlation from further processing:

$$c_n(x_o, y_o; \phi_n) = \frac{s_n(x_o, y_o; \phi_n) + |s_n(x_o, y_o; \phi_n)|}{2} \quad (3)$$

The algorithm continues with the doubled angle assignment and summation, which can be expressed in form:

$$\vec{c}(x, y) = \sum_n c_n(x_o, y_o; \phi_n) \cdot e^{j2\phi_n} \quad (4)$$

and, finally, the angle decrement:
 $\vec{v}(x, y) = |\vec{c}(x, y)| \cdot e^{j0.5 \text{Arg}(\vec{c}(x, y))} \quad (5)$

The acquired vectors smoothly follow the direction of the detected ridges, as shown in Figure 3 (up), but this is not always the case. More frequently, the palmprint images, which are used as forensic evidence, contain the ridge structure, that is hardly noticeable and is covered with noise, artifacts or crease of other direction. In this case the NH-CMF becomes useless, because it is aimed to detect

individual lines, not a set of overlapping lines (Figure 3 (down)). The possible application of NH-CMF in ridge tracking task in the field of forensics makes it an interesting challenge to adapt this algorithm to handle images, where differently oriented lines (ridges and crease) are overlapped, but must be detected separately.

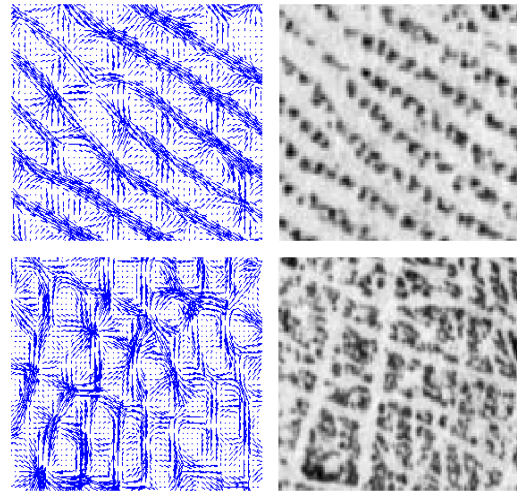


Fig. 3: NH-CMF result for different palmprint areas: with clear ridge structure (up), and overlapped with crease – a problematic area (down)

IV. DETECTION AND SEPARATION OF THE OVERLAPPING LINES

In the case of overlapping lines, NH-CMF detects all of them scattered around the image region. Therefore, statistical approaches can be used to analyze their significance and directions. For this task we use magnitude weighted angle histogram (MWAH). Suppose having a set of I vectors $\{v_i; i=1 \dots I\}$, where I is the pixel count in the analyzed image region. Let $|\vec{v}_i|$ be the magnitude of vectors, and $\text{Arg}(\vec{v}_i)$ be the floored angle (in degrees). The magnitude weighted angle histogram h can then be defined by the following equation:

$$h(k) = \sum_{v_i, \text{Arg}(\vec{v}_i) = k} |\vec{v}_i| \quad (6)$$

where k is the analyzed angle in degrees, $k=0 \dots 179$. Thus, we ensure that the vectors that have longest magnitude have biggest impact on the calculated histogram values. For non-problematic image regions, where clear pattern of similarly oriented ridges is present, the MWAH will always show one dominating peak, denoting the ridge flow direction (Fig. 4 (left)). For problematic regions, the MWAH presents multiple peaks (Fig. 4 (right)), each peak corresponds to the different LLO being overlapped. The analysis of MWAH peaks allows us to choose the preferred LLO direction as well as to know the direction and proportion of the unwanted details. We analyze MWAH for partially overlapping regions of 71×71 pixels, chosen as a tradeoff between computation speed and statistical precision of MWAH. Once the direction of interest, $\phi^*(x, y)$ is found (in radians), the detail rejection function $r(\phi)$ can be formulated, for example, as in (7).

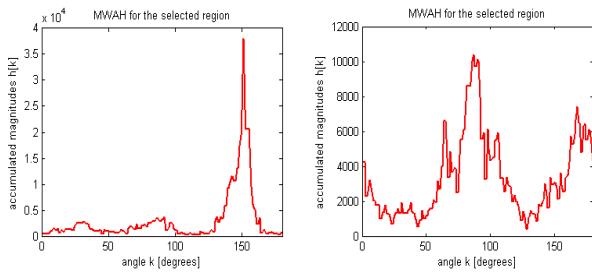


Fig. 4: MWAH for different type of image regions: clear ridge pattern with one direction (left), and problematic region with overlapping ridge and crease structures (right)

$$r(\phi - \phi'(x,y)) = \frac{r_{\max} - 1}{r_{\max}} \cdot \frac{\cos(2(\phi - \phi'(x,y))) + 1}{2} + \frac{1}{r_{\max}} \quad (7)$$

where r_{\max} is tunable unwanted detail rejection level (e.g. 64).

V. APPLIED ALGORITHM MODIFICATIONS

We leave matched filtering part of the NH-CMF algorithm, which is performed by (2) and (3), unchanged. Since the acquired values $c_n(x_o, y_o; \phi_n)$ represent the image fragment match with the filter kernel, and we don't need the details of unwanted angles to be matched, next thing we apply is the match rejection:

$$c_n(x_o, y_o; \phi_n) = r(\phi_n - \phi'(x,y)) \cdot c_n(x_o, y_o; \phi_n) \quad (8)$$

Further algorithm continues unchanged:

$$\vec{c}'(x,y) = \sum_n c_n(x,y; \phi_n) \cdot e^{j2\phi_n'} \quad (9)$$

$$\vec{v}'(x,y) = |\vec{c}'(x,y)| \cdot e^{j0.5} \cdot \text{Avg}(\vec{c}'(x,y)) \quad (10)$$

The result is *NH-CMF with angular preference*, and the preferred angle is defined by value $\phi'(x,y)$ for each pixel. The processing of an image consists of two steps:

A. The input image is processed with original NHCMF:

As a result the output image $\vec{v}(x,y)$ is acquired and analyzed with MWAH. The preferred angle $\phi'(x,y)$ for each image region is assigned, according to MWAH peaks. In our experiment, the highest peak's angle was automatically chosen.

B. The input image is processed again, using the modify:

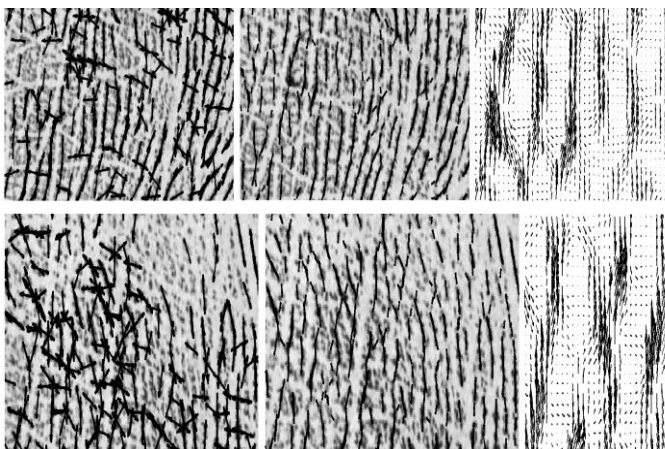


Fig. 5: Filtration result in the problematic region using NH-CMF (left), and modified NH-CMF in the same problematic region with automatic angular preference estimation using

MWAH (middle) – local maximums are shown in both cases, and matching intensity vectors (right), shown for the marked region

VI. RESULTS AND CONCLUSION

The method described in this paper shows how incorporating the NH-CMF and MWAH it is possible to improve the filtration result of a palmprint. Figure 5 shows the comparison of NH-CMF and proposed modified version of NH-CMF with angular preference. The output image $v'(x,y)$ shows the improvement of filtration quality over the original NH-CMF (Fig. 5 (middle) over Fig. 5 (left) and Fig. 5 (right) over Fig. 3 (down)). Using angular preference we are able to fine-tune filter performance to detect only details of interest, and after refiltering the image, some details that were not seen after first filtration become visible. However, when dealing with images of such low quality it is important to be careful with image processing methods, because false detections may occur, which is unacceptable in forensics.

ACKNOWLEDGEMENTS

This research is partially supported by ERSF project No.2010/0285/2DP/2.1.1.2.0/10/APIA/VIA/098

REFERENCES

- [1] S. Dewan and W. Elementary, "Scan a Palm, Find a Clue," *The New York Times*, 2003.
- [2] Jifeng Dai, and Jie Zhou, "Multi-feature Based High-resolution Palmprint Recognition," *Pattern Analysis and Machine Intelligence, IEEE Transactions on*, vol.33, no.5, pp.945-957, May 2011
- [3] Y. Punsawad, Y. Wongsawat, "Palmprint image enhancement using phase congruency," *IEEE International Conference on Robotics and Biomimetics, 2008. ROBIO 2008.*, vol., no., pp.1643-1646, 22-25 Feb. 2009
- [4] W.W. Boles, S.Y.T. Chu, "Personal identification using images of the human palms," in: *Proceedings of IEEE Region 10 Annual Conference, Speech and Image Technologies for Computing and Telecommunications*, vol. 1, 1997, pp. 295-298.
- [5] X. Wu, K. Wang, D. Zhang, "Wavelet based palmprint recognition," *Proceedings of the First International Conference on Machine Learning and Cybernetics*, vol.3, 2002, pp. 1253-1257.
- [6] Y. Li, K. Wang, D. Zhang, "Palmprint recognition based on translation invariant Zernike moments and modular neural network," *Lecture Notes in Computer Science*, Springer, vol.3497, 2005, pp. 177-182.
- [7] Koichi Ito, Takafumi Aoki, Hiroshi Nakajima, Koji Kobayashi, and Tatsuo Higuchi. "A Palmprint Recognition Algorithm Using Phase-Only Correlation," *IEICE Trans. Fundam. Electron. Commun. Comput. Sci.* E91-A, 4 (April 2008), 1023-1030.
- [8] Jain, A.K.; Jianjiang Feng; , "Latent Palmprint Matching," *Pattern Analysis and Machine Intelligence, IEEE Transactions on*, vol.31, no.6, pp.1032-1047, June 2009

- [9] Wai Kin Kong, David Zhang, Wenxin Li, "Palmprint feature extraction using 2-D Gabor filters," *Pattern Recognition*, Volume 36, Issue 10, October 2003, Pages 2339-2347,
- [10] Pudzs, M.; Greitans, M.; Fuksis, R.; , "Complex 2D matched filtering without Halo artifacts," *Systems, Signals and Image Processing (IWSSIP), 2011 18th International Conference on* ,vol., no., pp.1-4, 16-18 June 2011
- [11] Greitans, M.; Pudzs, M.; Fuksis, R.; , "Object analysis in images using complex 2D matched filters," *EUROCON 2009,EUROCON '09. IEEE* , vol., no., pp.1392-1397, 18-23 May 2009
- [12] Rihards Fuksis, Modris Greitans, and Mihails Pudzs."Processing of palm print and blood vessel images for multimodal biometrics," In *Proceedings of the COST 2101 European conference on Biometrics and ID management (BioID'11)*,Springer-Verlag, Berlin, Heidelberg, 238-249.

